

# Thermal Degradation of Type I Collagen from Bones

M. L. Lambri<sup>1,2</sup>, E. D. Giordano<sup>2,3</sup>, P. B. Bozzano<sup>4</sup>, F. G. Bonifacich<sup>2</sup>, J. I. Pérez-Landazábal<sup>5,6</sup>, G. I. Zelada<sup>2</sup>, D. Gargicevich<sup>2</sup>, V. Recarte<sup>5,6</sup> and O. A. Lambri<sup>2\*</sup>

<sup>1</sup>Faculty of Humanities and Arts, National University of Rosario, Rosario, Argentina

<sup>2</sup>CONICET–UNR, Materials Laboratory, School of Electrical Engineering, Center for Technology and Electrical Research, Faculty of Exact Sciences, Engineering and Land Surveying, Avda. Pellegrini 250, 2000 Rosario, Argentina

<sup>3</sup>CONICET–UNR, Area of Chemical Technology, Faculty of Biochemical and Pharmaceutical Sciences, Rosario, Argentina

<sup>4</sup>Electron Microscopy Laboratory, Materials Activity Unit, Constituyentes Atomic Center, National Atomic Energy Commission and the Institute Sabato – National University of San Martín, Avda. Gral Paz 1499, (1650) San Martín, Argentina

<sup>5</sup>Department of Physics, Public University of Navarra, Campus de Arrosadía, 31006 Pamplona, Spain

<sup>6</sup>Institute for Advanced Materials (INAMAT), Public University of Navarra, Campus de Arrosadía, 31006 Pamplona, Spain

Received January 28, 2016; Accepted May 10, 2016

**ABSTRACT:** The denaturation processes of collagen in the temperature range between 450 K and 670 K are revealed through studies performed on cow rib bones by means of mechanical spectroscopy, differential scanning calorimetry, thermogravimetry, scanning electron microscopy and infrared spectroscopy. The conformational change of the collagen molecules from a triple helix structure to a random coil was found at around 510 K. It was determined that the transformation is developed through the viscous movement of fibrils with an activation energy of  $(127 \pm 8)$  kJ/mol. The second stage of massive bulk deterioration of the collagen was found at around 600 K, which leads to the loss of the mechanical integrity of the bulk collagen. In addition, an easy-to-handle viscoelastic procedure for obtaining the activation energy of the denaturation process from mechanical spectroscopy studies was also shown.

**KEYWORDS:** Archaeometry, bone repair, thermal denaturation, tissue engineering, type I collagen

## 1 INTRODUCTION

There is great interest in the clinical and medical communities focused on the reconstruction, repair, and replacement of bones, given the frequency and importance of pathological situations. Collagen, which is an essential component of natural bone, plays a pivotal role in the formation of the biological scaffold for tissue engineering [1, 2]. In addition, a considerable number of studies have also been performed in the field of archaeometry, archaeology and palaeontology, focused on the aging processes of bone and collagen, which ultimately lead to the processes of mineralization and fossilization [3–5].

The collagen molecule consists of triple helical tropocollagen molecules at nanometric scale. Staggered arrays of collagen molecules form fibrils, which arrange to form the collagen fibers [6] where the

carbonated apatite crystals (“dahllite”) are embedded, giving rise to the bone [7, 8].

It should be highlighted that in clinical and medical communities the temperature at which collagen denatures from a triple helix to a random coil structure is a useful measure of the degree of both crosslinking and crystallinity. The denaturation temperature and solubilization characteristics of collagen have been important tools in the study of maturation and of molecular defects linked with connective tissue diseases. In addition, the study of the denaturation behavior of collagen is crucial in order to stabilize the collagen against breakdown and resorption by enzymatic chain scission in “*in-vivo*” long-term applications of biomaterials [1, 2, 6–10].

Besides, in archaeometry, archaeology and palaeontology, the denaturation processes related to the triple helix transition present high interest, for instance, in order to infer from buried and/or burned bones the behavior and habits of people who once inhabited archaeological sites [3, 4, 11].

In previous works the biodegradation of collagen by denaturation of albumin and hemoglobin proteins,

\*Corresponding author: olambri@fceia.unr.edu.ar

the loss of water and the loss of crystallization water during warming up to around 500 K, have been studied [12, 13].

In the present work, the denaturation processes of collagen in the temperature range between 450 K and 670 K were revealed through studies performed on cow rib bones by means of mechanical spectroscopy (MS), differential scanning calorimetry (DSC), thermogravimetry (TGA), scanning electron microscopy (SEM) and infrared spectroscopy (IR). In fact, the temperature for studying the denaturation processes was increased over 450 K, with regard to the previous works, in order to allow the study of the deterioration of the triple helix and the final bulk degradation of the collagen solid proteins.

The aim of the present work is to show that the deterioration of the collagen from cow rib bones at temperatures above 450 K is composed of two stages of denaturation at around 510 K and 600 K. Their related physical-chemical mechanisms of denaturation are discussed. In addition, an easy-to-handle viscoelastic procedure was applied for obtaining the activation energy of the denaturation process at 510 K from MS studies. Indeed, it represents an important tool for the study of the physical-chemical processes related to the denaturation of collagen viewed through a very sensitive technique such as MS.

## 2 EXPERIMENTAL

### 2.1 Samples

The studied bones were ribs of fresh cow meat purchased from three different providers. Samples were taken from bones by cutting with a jeweler's saw in perpendicular direction to their longest dimensions (see ref. [12] for more details). Three samples from the bone of each provider were taken. In MS and IR studies, composite-type samples, including both the cortical and cancellous parts, were used. For MS and IR, the samples were in a parallelepiped shape of around 3 mm × 4 mm × 40 mm, the final size being reached by means of mechanical polishing. For DSC and TGA studies, due to the size of the sample holder of the equipment, the use of samples made only of cortical or cancellous parts was required.

### 2.2 Measurements

The MS studies, which involve the simultaneous measurement of damping ( $\tan(\phi)$ ) and natural oscillating frequency ( $f$ ) as a function of temperature ( $T$ ) [14], were performed at different frequencies between 5 and 40 Hz, within the temperature range

from 250 K up to 670 K. Tests were carried out in torsion, under pure argon atmosphere at standard pressure. The heating and cooling rates were of 1 K/min. The maximum shear strain on the sample was  $2 \times 10^{-4}$ . The error for damping and  $f^2$  (which is proportional to the dynamic modulus) was less than 2%. DSC measurements at a heating/cooling rate of 10 K/min were carried out in TA Q100 DSC equipment under nitrogen atmosphere. The weight loss (TGA, BOECO balance with a precision of 0.1 mg) was obtained after a heating/cooling process at 2 K/min up to different maximum temperatures,  $T_m$ , in an argon atmosphere. The weight loss was determined as  $\rho = (w_i - w(T_m))/w_i$ , where  $w_i$  is the initial weight at room temperature (RT) and  $w(T_m)$  is the weight measured at RT after a cycle reaching a maximum  $T_m$  temperature. The error in the measured points was less than 0.02%. SEM studies were performed in a FEI Quanta 200 scanning electron microscope operated at 15 kV, under vacuum. IR studies were carried out in a Shimadzu Prestige 21, FTIR spectrometer, with an attenuated total reflectance (ATR) accessory. Forty scans per spectrum, in the wavenumber range of 4000–400  $\text{cm}^{-1}$  with a resolution of 4  $\text{cm}^{-1}$ , were used for each studied sample.

## 3 RESULTS AND DISCUSSION

Figure 1a shows the damping curves for bone samples measured at different oscillating frequencies during warming within the temperature interval from 450 K up to 673 K. The MS measurements were performed up to 673 K, since the apatite is stable up to this temperature [10, 15]. For the case of the sample measured at low frequency the cooling run in temperature is also shown. A damping peak with a height of about  $8 \times 10^{-2}$  appears during warming at around 510 K, labeled as (1), which is independent of the oscillating frequency, i.e., the peak temperature (temperature where the maximum damping occurs) does not shift with a change in the oscillating frequency. Besides, a dependence of the strength of the (1)-peak (peak height) as a function of frequency cannot be clearly determined. The lack of resolution of the relaxation strength regarding the oscillation frequency could be related to the error bandwidth found in bone measurements, as will be mentioned in the following paragraphs. However, it should be pointed out that the non-dependence of the strength of (1)-peak as a function of oscillating frequency is in agreement with a first order transition process (except for martensitic transitions). In fact, a dependence of the damping peak strength on the oscillating frequency can be expected in studies of higher-order phase transitions

[14, 16, 17]. In addition, a group of damping peaks can also be seen at around 600 K, labeled as (2), which do not exhibit a clear dependence of the strength and the peak temperature upon the oscillating frequency. Then, peaks (1) and (2) are not related to a thermally activated phenomenon involving an Arrhenius-type law of relaxation times. In contrast, they can be related to critical phenomena which develop at around 510 K and 600 K. Moreover, the damping curves do not exhibit relaxation processes during the cooling down, after warming up to 670 K, which indicates that peaks (1) and (2) are related to irreversible thermodynamic processes.

The behavior of  $f^2$  for curves plotted in Figure 1a is shown in Figure 1b. A step-down was measured within the temperature interval where the development of (1)-peak takes place. In contrast, for the temperature interval of the (2)-peak an increase followed by a decrease was measured.

The measured curves of damping and modulus for samples taken from different ribs, in the temperature intervals of the (1)- and (2)-peaks, exhibited a discrepancy of around 15% and 50%, respectively. The discrepancy in damping and modulus of around 15% for the (1)-peak is in agreement with previous works [12, 13]. The large discrepancy occurring for the (2)-peak is related to the physical-chemical mechanism controlling this relaxation, as will be shown in the following paragraphs. Nevertheless, the general trends of the curves for damping and modulus are completely similar and reproducible.

### 3.1 The Denaturation Process at Around 510 K

A first-order phase transition which occurs at a given temperature leads to changes in both the damping and

the elastic modulus of the sample under study. It was reported that for describing the  $\tan(\phi)$  peak promoted by a first-order phase transition, an analytical expression of standard anelastic solid type can be used by considering an appropriate relaxation time [16]. The relaxation time will exhibit a law more complicated than a simple Arrhenius behavior. Then, the expression for  $\tan(\phi)$  can be written as [16, 18–20]

$$\tan(\phi) = a \frac{\omega\tau}{1 + (\omega\tau(T, \xi_i))^2} = \frac{a}{2 \cosh[\ln(\omega\tau(T, \xi_i))]} \quad (1)$$

where  $a$  is related to the relaxation strength of the process,  $\omega = 2 \cdot \pi \cdot f$  is the angular frequency and  $\tau(T, \xi_i)$  is an appropriate relaxation time of the process which contains information on the internal physical-chemical variables of the transformation,  $\xi_i$ , in the form

$$\tau(T, \xi_i) = \tau_0^*(T, \xi_i) \exp\left(\frac{H}{kT}\right) \quad (2)$$

with  $\tau_0^*(T, \xi_i)$  the pre-exponential factor which involves information on the phase transition process,  $k$  the Boltzmann constant and  $H$  the activation energy of the process.

By combining Equations 1 and 2, it can be written

$$\ln \tau_0^*(T, \xi_i) + \frac{H}{kT} = \cosh^{-1}\left(\frac{2 \tan(\phi)_p}{2 \tan(\phi)}\right) - \ln \omega \quad (3)$$

where  $a = 2 \cdot \tan(\phi)_p$ , with  $\tan(\phi)_p$  the value of the damping at the maximum of the peak, comes from the usual normalization condition of the damping peak [14, 16, 18, 19]. By calling the right term  $\Psi = \cosh^{-1}(2 \tan(\phi)_p / 2 \tan(\phi)) - \ln \omega$ ,  $H$  can be easily obtained from a plot of  $\Psi$  as a function of  $1/T$ . For the calculations, the low temperature tail of (1)-peak was only used, since the high temperature tail exhibits a

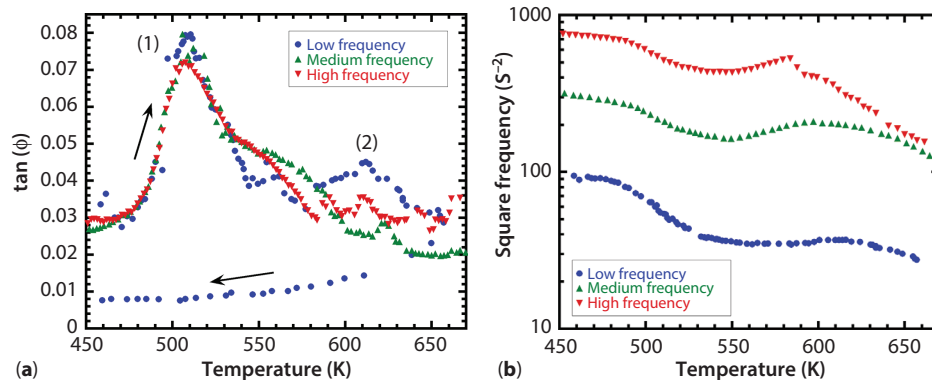


**Figure 1** (a) Damping ( $\tan(\phi)$ ) as a function of temperature for bone composite-type samples (cortical plus cancellous parts). Arrows indicate the warming and cooling runs. (b) Square frequency (proportional to the dynamic shear modulus) as a function of temperature for the spectra from Figure 1a.

hump which could be related to the overlap of other relaxation processes. This hump could be related to the start of the peaks group labeled as (2). Figure 2 shows the  $\psi$  vs.  $1/T$  plot for the peak measured at high frequency from Figure 1a. The  $\psi$  vs.  $1/T$  plots were constructed for the whole group of nine samples, resulting in an average value of  $H = (127 \pm 8)$  kJ/mol. The ordinate cut value does not reveal a direct physical meaning, due to the mode of constructing the relaxation time [18, 20]. In fact, the contribution of the internal variables of the transformation is located at the pre-exponential factor. Moreover, it could also contain the information about the distribution function of relaxation times [18, 20].

It should be highlighted that a value of  $H = 130$  kJ/mol was measured, from MS measurements performed as a function of frequency at different temperatures, for the movement of collagen fibers in dry bones [21]. Therefore, it can be proposed that (1)-peak involves the movement of collagen fibrils in the dry bone. The state of dehydrated collagen can be assured from previous works using MS, DSC, TGA and SEM studies, where both the free water and the crystallization water were already eliminated at temperatures over 450 K [12]. In addition, the non-appearance of relaxation process after warming up to 670 K and the temperature of appearance of (1)-peak suggest that the driving force controlling the relaxation process is the conformational changes of the collagen molecules from a triple helix structure to a random coil (TP  $\rightarrow$  RC) [6]. In fact, during denaturation, collagen fibrils undergo several conformational changes caused by the breaking of different crosslinks present at the intermolecular level, such as the nonenzymatic glycosylation of lysine and hydroxylysine residues, and at the intramolecular level, such as the disulphide bridges. In addition, the

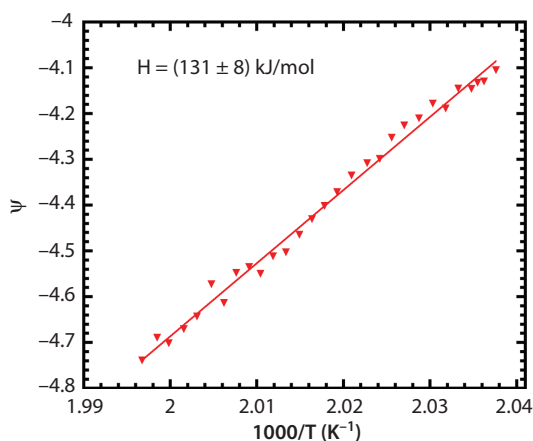


**Figure 2** The  $\psi$  vs.  $1/T$  plot obtained for the spectrum measured at high frequency from Figure 1a. See explanation in the text.

H-bonded water involved in stabilizing the collagen molecule is released, leading to the collapse of the triple helix structure of the molecules [6].

The appearance of TP  $\rightarrow$  RC transformation at around 510 K could also be reinforced from TGA and DSC studies, as shown in Figure 3. A small reduction in weight of around 3% is recorded from TGA studies at temperatures where the TP  $\rightarrow$  RC transformation develops (see Figure 3). This weight loss could be related to the evaporation of residual strongly bound water and the liberation of low molecular products of the thermal degradation of the scaffold [1]. These products could be carbon dioxide (from a decarboxylation reaction of amino acids), pyrrole derivatives, pyrrolidine derivatives, nitriles and amides [22–24].

Moreover, thermograms reveal two small endothermic reactions at around 510 K, for both cortical and cancellous parts of the rib bones, which are related to the evaporation of residual strongly bound water and the continuation of the conformational changes of superhelix [1]. The small intensity of these reactions leads to an unclear determination of the baseline for this temperature range, impeding the obtainment of the activation energy from the DSC test. Therefore, we can establish that the (1)-peak is related to the TP  $\rightarrow$  RC transformation, where the movement of fibrils in a viscous mode occurs; involving an activation energy of  $(127 \pm 8)$  kJ/mol.

### 3.2 The Denaturation Process at Around 600 K

The viscoelastic procedure described in Section 3.1 to obtain  $H$  cannot be applied for the (2)-peak because it involves the overlapping of several peaks. Nevertheless, the temperature interval for the

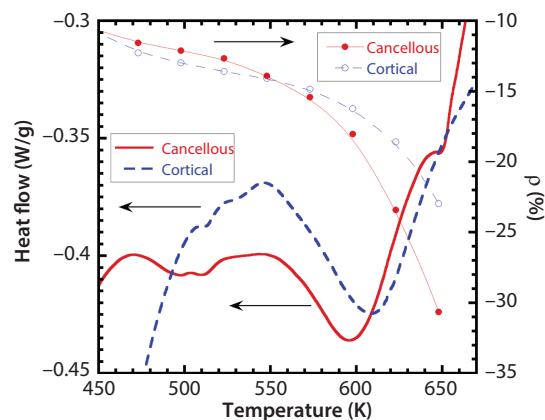


**Figure 3** Left axis: DSC thermograms for cortical (dashed line) and cancellous (full line) parts of a bone sample. Right axis: TGA behavior for cortical (empty symbols) and cancellous (full symbols) parts of a bone sample.

development of the (2)-peak is in good correspondence with both the marked decrease in weight in the TGA curves, right axis in Figure 3, and the endothermic reaction at around 600 K in the DSC test, left axis in Figure 3. From the thermograms of Figure 3, it is complicated to obtain the activation energy of the endothermic reaction at around 600 K owing to the non-determination of the baseline. It is possible that some contribution of the peaks related to the TP  $\rightarrow$  RC transformation is superimposed on the reaction at 600 K.

The marked fall of the weight for temperatures higher than 550 K from TGA studies (right axis in Figure 3) and the decrease in the values of the moduli from 600 K upwards (Figure 1b), indicate that a massive bulk deterioration of the bone samples develops, which is in agreement with previous works [3, 6]. The present bulk deterioration of the sample gives rise to the difference in damping values within the zone of the (2)-peak among different samples, due to the random evolution of the mesostructure involved during this subsequent deterioration.

The bulk degradation, which is a subsequent stage of deterioration of the collagen fibers, was also checked from SEM and IR studies. The SEM micrographs performed on samples after a heating up to 673 K reveal the shrinkage of the mesostructure related to the massive bulk degradation of the fibers (Figure 4). The mesostructure exhibits both large cracks and empty regions, which were absent in the sample prior to the thermal treatment, as was shown in previous works [12]. In addition, the degree of compactness and cracking of the mesostructure is larger in the samples

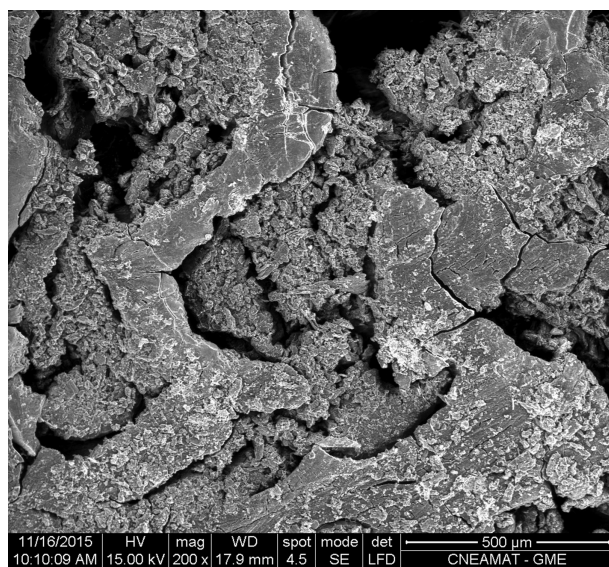


**Figure 4** SEM micrograph of a cancellous part of bone sample after heating up to 670 K.

heated up to 670 K than in samples heated up to 420 K (see more details in ref. [12]), as could be expected.

Figure 5 shows the normalized infrared absorbance for a bone sample, both in the fresh state and after heating up to 673 K. The most intense peaks in the spectrum at 557, 599 and 1013  $\text{cm}^{-1}$  are related to the bending and stretching vibrations of  $\text{PO}_4^{3-}$  from the apatite [25]. Spectra were normalized in regard to the peak of the apatite at 1013  $\text{cm}^{-1}$ . Indeed, the most intense peak at 1013  $\text{cm}^{-1}$  corresponds to the stretching vibrations of  $\text{PO}_4^{3-}$  in the apatite, which shows a high stability below 1073 K. This is supported by the unaltered presence of  $\text{CO}_3^{2-}$  groups at 871  $\text{cm}^{-1}$ . However, annealing above 1073 K can remove this carbonate group, revealing a decomposition of the apatite [15]. Besides, in our FTIR studies the fresh and the annealed samples were taken from the same bone. Consequently, in order to compare the behavior of thermal denaturation of collagen due to warming up to 673 K, normalizing the peak at 1013  $\text{cm}^{-1}$  seems to be the more appropriate procedure. Moreover, for samples taken from different ribs, the same trend and behavior of the FTIR spectra related to the thermal denaturation were recorded.

After a heating up to 673 K, it can be seen that the FTIR spectrum shows a decrease in the intensity of the peaks related to the Amide I, II and III at 1633, 1541, 1444, and 1409  $\text{cm}^{-1}$  [26]. In fact, there is not only a decrease of the intensity, but also, the shape of the peaks is a bit different between both samples. In contrast, the intensity of the peaks related to the apatite does not show any change after warming up to 673 K, in agreement with the above-exposed and previous works [10, 15].

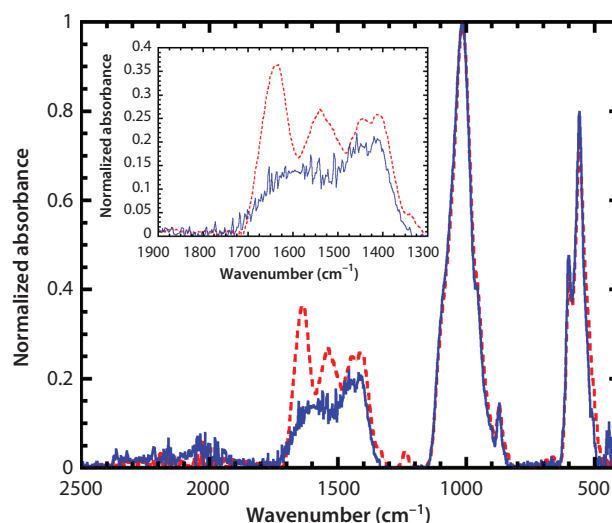


**Figure 5** FTIR spectra for a composite-type sample prior to (dashed line) and after a heating up to 670 K (full line). Inset: Magnification zone between 1900 and 1300  $\text{cm}^{-1}$ .

Therefore, the (2)-peak at around 600 K can be related to a subsequent stage of denaturation of the collagen fibers.

## 4 CONCLUSIONS

Two denaturation processes of type I collagen were determined in the temperature range between 450 K and 670 K, through studies performed on cow rib bones. The conformational changes of the collagen molecules from a triple helix structure to a random coil were found at around 510 K. In addition, from an easy-to-handle mathematical viscoelastic procedure, it was determined that the conformational changes are made through the viscous movement of fibrils, invoking an activation energy of  $(127 \pm 8)$  kJ/mol. A subsequent stage of massive bulk deterioration of the collagen was found at around 600 K which leads to the loss of the mechanical integrity of the bulk collagen.

## ACKNOWLEDGMENTS

This work was partially supported by the CONICET-PIP No. 179CO and 2098, the PID-UNR ING 450 and ING 453 (2014-2017) and the Collaboration Agreement between the Universidad Pública de Navarra and the Universidad Nacional de Rosario, Res. 3247/2015.

## References

1. K. Pietrucha, Changes in denaturation and rheological properties of collagen-hyaluronic acid scaffolds as a result of temperature dependencies. *Int. J. Biol. Macromol.* **36**, 299–304 (2005).
2. E.B. Garner, R. Lakes, T. Lee, C. Swan, and R. Brand, Viscoelastic dissipation in compact bone: Implications for stress-induced fluid flow in bone. *J. Biomech. Eng.* **122**, 166–172 (2000).
3. M. Tomassetti, F. Marini, L. Campanella, and A. Coppa, Study of modern or ancient collagen and human fossil bones from an archaeological site of middle Nile by thermal analysis and chemometrics. *Microchem. J.* **108**, 7–13 (2013).
4. G. Piga, A. Santos-Cubedo, A. Brunetti, M. Piccinini, A. Malgosa, E. Napolitano, and S. Enzo, A multi-technique approach by XRD, XRF, FT-IR to characterize the diagenesis of dinosaur bones from Spain. *Palaeogeogr. Palaeoclimatol. Palaeoecol.* **310**, 92–107 (2011).
5. T. Tütken and T.W. Vennemann, Fossil bones and teeth: Preservation or alteration of biogenic compositions? *Palaeogeogr. Palaeoclimatol. Palaeoecol.* **310**, 1–138 (2011).
6. L. Bozec and M. Odlyha, Thermal denaturation studies of collagen by microthermal analysis and atomic force microscopy. *Biophys. J.* **101**, 228–236 (2011).
7. M. Lau, K. Lau, H. Ku, F. Cardona, and J. Lee, Analysis of heat-treated bovine cortical bone by thermal gravimetric and nanoindentation. *Compos. Part B-Eng.* **55**, 447–452 (2013).
8. J.F. Mano, Viscoelastic properties of bone: Mechanical spectroscopy studies on a chicken model. *Mat. Sci. Eng. C.* **25**, 145–152 (2005).
9. J.M. Lee, C.A. Pereira, D. Abdulla, W.A. Naimark, and I. Crawford, A multi-sample denaturation temperature tester for collagenous biomaterials. *Med. Eng. Phys.* **17**, 115–121 (1995).
10. L. Kubisz and S. Mielcarek, Differential scanning calorimetry and temperature dependence of electric conductivity in studies on denaturation process of bone collagen. *J. Non-Cryst. Solids* **351**, 2935–2939 (2005).
11. M.C. Stiner, S.L. Kuhn, S. Weiner, and O. Bar-Yosef, Differential burning, recrystallization, and fragmentation of archaeological bone. *J. Archaeol. Sci.* **22**, 223–237 (1995).
12. O.A. Lambri, J.I. Pérez-Landazábal, F.G. Bonifach, V. Recarte, M.L. Lambri, G.I. Zelada, F. Tarditti, and D. Gargicevich, Damping micromechanisms for bones above room temperature. *J. Biomim. Biomater. Tissue Eng.* **19**, 87–98 (2014).
13. M.L. Lambri, J.I. Pérez-Landazábal, V. Recarte, F. Tarditti, and O.A. Lambri, Effect of the mesostructure on the mechanical dynamical behaviour in cancellous bones. *Acta Microsc.* **22**, 26–31 (2013).
14. R. Schaller, G. Fantozzi, and G. Gremaud (Eds.), *Mechanical Spectroscopy*, Trans. Tech. Publications Ltd., Switzerland (2001).
15. C.Y. Ooi, M. Hamdi, and S. Ramesh, Properties of hydroxyapatite produced by annealing of bovine bone. *Ceram. Int.* **33**, 1171–1177 (2007).
16. A.S. Nowick and B.S. Berry, *Anelastic Relaxation in Crystalline Solids*, Academic Press, New York, NY (1972).
17. R.K. Pathria, *Statistical Mechanics*, Pergamon Press, Oxford, UK (1977).
18. O.A. Lambri, New procedure for determining internal friction parameters of tension-induced relaxation processes with distribution of relaxation times. *Mater. Trans. JIM.* **35**, 458–465 (1994).
19. O.A. Lambri, C.L. Matteo, R.R. Mocellini, P.A. Sorichetti, and G.I. Zelada-Lambri, *Propiedades Viscoelásticas y Eléctricas de Sólidos y Líquidos. Una Introducción a la Electro-Reología con sus Aplicaciones Tecnológicas*, Editora de la Universidad Nacional de Rosario, Rosario (2008).
20. G.I. Zelada, Mecanismos de interacción dislocaciones – Defectos puntuales en molibdeno a temperaturas entre 300–1300 K (0.3 Tf), PhD. Thesis, Universidad Nacional de Rosario, Argentina (2008).
21. R. Schaller, S. Barrault, and P. Zysset, Mechanical spectroscopy of bovine compact bone. *Mat. Sci. Eng. A.* **370**, 569–574 (2004).
22. A. Adamiano, Pyrolysis of peptides and proteins: Analytical study and environmental applications, PhD. Thesis, Università di Bologna (2012).
23. Z. Sebestyén, Z. Czégény, E. Badea, C. Carsote, C. Sendrea, E. Barta-Rajnai, J. Bozi, L. Miu, and E. Jakab,



- Thermal characterization of new, artificially aged and historical leather and parchment. *J. Anal. Appl. Pyrolysis* **115**, 419–427 (2015).
24. A. Adamiano, D. Fabbri, G. Falini, and M. Giovanna Belcastro, A complementary approach using analytical pyrolysis to evaluate collagen degradation and mineral fossilisation in archaeological bones: The case study of Vicenne-Campochiaro necropolis (Italy). *J. Anal. Appl. Pyrolysis*, **100**, 173–180 (2013).
  25. N. Kourkoumelis, A. Lani, and M. Tzaphlidou, Infrared spectroscopic assessment of the inflammation-mediated osteoporosis (IMO) model applied to rabbit bone. *J. Biol. Phys.* **38**, 623–635 (2012).
  26. M.M. Figueiredo, J.A.F. Gamelas, and A.G. Martins, Characterization of bone and bone-based graft materials using FTIR spectroscopy: Infrared Spectroscopy, in *Life and Biomedical Sciences*, T. Theophanides (Ed.), pp. 315–339, InTech, Rijeka, Croatia (2012).